Electronic Supplementary Material (ESI) for Sustainable Energy & Fuels.
This journal is © The Royal Society of Chemistry 2020

Electronic Supplementary Information

Plasma-reduced $Co(OH)_2$ with activated hydrogen evolution and overall water splitting performance

Junxiang Jiang,[a]† Yuanhao Tang,[a]† Lin Dong,[b] Wenhao Zhang,*[ac] Haobin Wu,[a] and Xin-Yao Yu*[ab]

[a]*School of Material Science and Engineering, Zhejiang University, Hangzhou, 310027, P. R. China.*

[b]*Institutes of Physical Science and Information Technology, Anhui University, Hefei, 230601, P. R. China. Email: yuxinyao@ahu.edu.cn*

[c]*School of Chemistry and Chemical Engineering, Ocean University of China, Qingdao, 266100, P. R. China. Email: wenhao2526@163.com*

†These two authors contribute equally to this work.

Experimental Section

Materials

Nickel foam (NF) with a thickness of 0.5 mm was purchased from Taiyuan Liyuan lithium Technology Co., Ltd. Carbon paper (CP) was purchased from Shanghai He Sen Electric Co., Ltd. Cobalt nitrate hexahydrate was purchased from Aladdin Reagent Co., Ltd. Potassium hydroxide and hydrochloric acid were purchased from Sinopharm Chemical Reagent Co., Ltd. Nafion (5 wt. %) was purchased from Sigma-Aldrich.

Preparation of $Co(OH)_2$ nanosheet arrays

NF and CP were employed as substrates for the electrodeposition. Before electrodeposition, the NF and CP were first ultrasonically cleaned in water and ethanol, followed by being cleaned in 2 M HCl to remove the surface oxide layer. Then, the cleaned NF was rinsed several times with water and ethanol and finally dried at 70 ℃. The $Co(OH)_2$ nanosheets were electrodeposited on NF or CP in a 0.05 M $Co(NO_3)_2$ solution with a deposition potential of -1.0 V (*vs*. saturated calomel electrode) and a deposition time of 20 min. A high precision electronic balance was used to determine the loading amount of the deposited $Co(OH)_2$. The average mass loading was approximately 3.0166 mg cm^{-2}.

Preparation of P-$Co(OH)_2$ nanosheet arrays

The NF or CP covered with precursor material was put into the chamber of a PECVD device and reduced by H_2/Ar plasma with the volumetric ratio of 1:9, the gas pressure of 40 Pa and RF power of 400 W for 20 min. The mass loading of P-$Co(OH)_2$ was 1.868 mg cm^{-2}.

Preparation of Co nanosheet arrays

The Co nanosheet arrays were obtained by calcinating $Co(OH)_2$ at 450 ℃ under a Ar/H_2 (v/v: 9/1) atmosphere for 3 h with a heating rate of 2 ℃ min^{-1}.

Preparation of CoO nanosheet arrays

The CoO nanosheet arrays were obtained by heating $Co(OH)_2$ at 600 ℃ in vacuum for 10 h with a heating rate of 5 ℃ min^{-1}.

Preparation of Pt/C electrode

A slurry was first prepared by dispersing 40 mg of Pt/C into a mixed solution of 20 μL Nafion, 0.5 mL water, and 0.5 mL ethanol for at least 30 minutes. Then, a certain volume of slurry was drop-casted on NF and then dried at 60 ℃. The mass loading of Pt/C is fixed at 1.868 mg cm^{-2}.

Materials characterizations

The morphologies and structures were characterized by scanning electron microscopy (SEM, Hitachi SU 8010), transmission electron microscopy (TEM, TF 20), high-resolution transmission electron microscopy (HRTEM), and selected area electron diffraction (SAED) (TF 20). The structure information was obtained from X-ray diffraction (XRD) (PANnalytical empyrean). All the samples tested in XRD were grown on the carbon paper to exclude the influence of metal nickel from NF. The detailed composition information was obtained from X-ray photoelectron spectroscopy (XPS, ThermoFischer ESCALAB 250 Xi). All the XPS data was calibrated by shifting the C 1s peak to 284.6 eV. The electronic environment around the atoms was detected by Electron Paramagnetic Resonance (EPR, Bruker A300) at room temperature and atmosphere pressure.

Electrochemical characterizations

The electrocatalytic tests were conducted in a standard three-electrode cell in 1.0 M KOH (pH = 13.85) using a CHI 760E electrochemistry workstation. A carbon rod was used as counter electrode. And the reference electrode is Hg/HgO electrode. The pristine $Co(OH)_2$, P-$Co(OH)_2$, Pt/C, and bare Ni foam were directly used as working electrodes. All the potentials were calibrated to the reversible hydrogen electrode (RHE). During HER tests, linear sweep voltammogram (LSV) curves were recorded from -0 to -0.5 V *vs*. RHE at a scan rate of 2 mV s^{-1}. Electrochemical impedance spectroscopy (EIS) test was performed in the frequency range of 10^4 to 0.1 Hz at an overpotential of 100 mV. Chronoamperometry (CA) tests were conducted at a constant overpotential of 68 mV for P-$Co(OH)_2$. The electrochemical double-layer capacitance (C_{dl}) was used to determine the electrocatalytic active surface area (ECSA). The C_{dl} was measured at scan rates of 20, 40, 60 and 80 mV s^{-1} in a non-Faradaic region from 0.05 to 0.15 V *vs*. RHE. Mass activity of as-synthesized electrocatalysts were determined according to the following equation.

$$Mass\ activity = \frac{j}{m}$$

m: the loading mass of electrocatalyst.

j: the measured current density (mA cm^{-2}) at the overpotential of 100 mV.

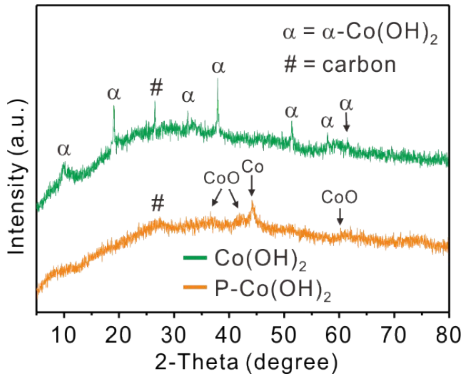

Fig. S1 XRD patterns of $Co(OH)_2$ and P-$Co(OH)_2$.

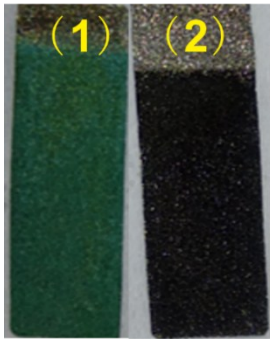

Fig. S2 The optical photograph of (1) $Co(OH)_2$ and (2) P-$Co(OH)_2$.

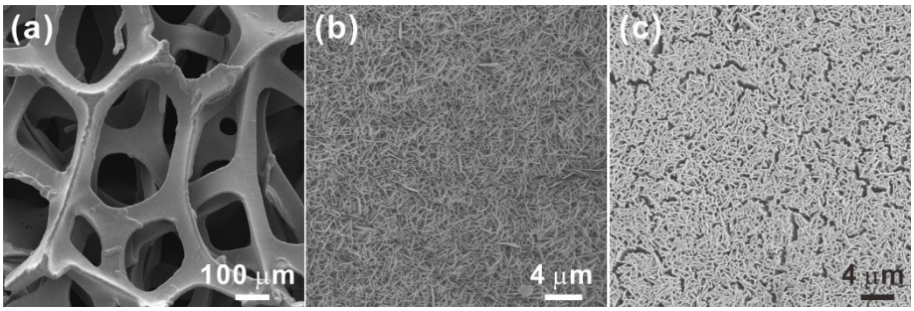

Fig. S3 SEM images of (a) blank Ni foam, (b) $Co(OH)_2$, and (c) P-$Co(OH)_2$.

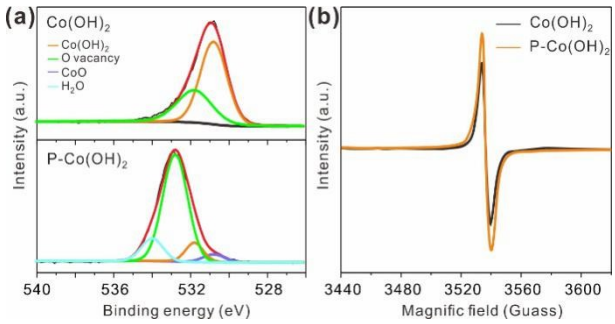

Fig. S4 (a) O 1s XPS spectra and (b) EPR spectra of $Co(OH)_2$ and P-$Co(OH)_2$.

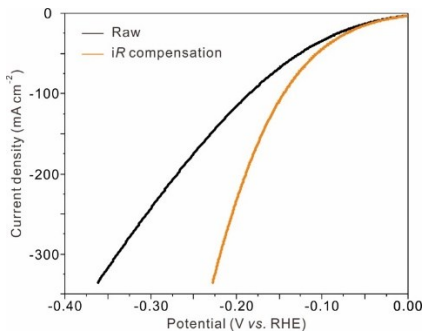

Fig. S5 LSV curves of P-$Co(OH)_2$ with and without i*R* compensation.

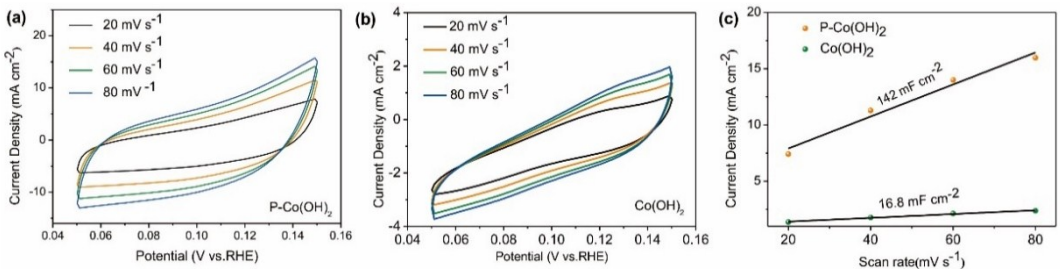

Fig. S6 Cyclic voltammogram curves of (a) P-$Co(OH)_2$ and (b) pristine $Co(OH)_2$ in the double layer capacitive region at different scan rates. (c) Capacitive currents as a function of scan rates fitted to a linear regression for P-$Co(OH)_2$ and $Co(OH)_2$.

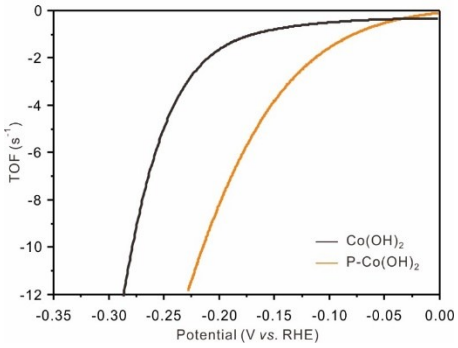

Fig. S7 TOF plots of $Co(OH)_2$ and P-$Co(OH)_2$.

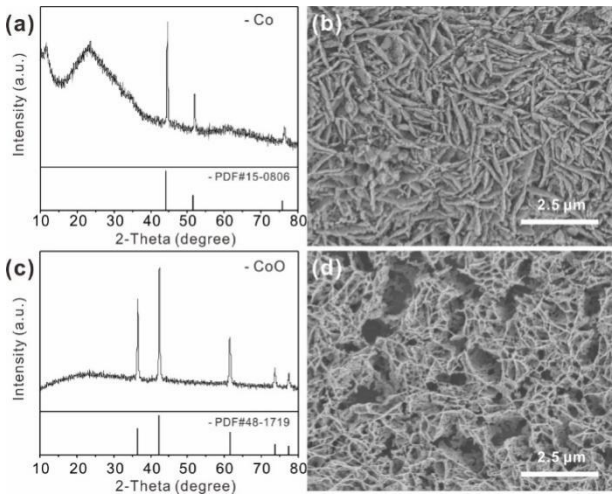

Fig. S8 XRD patterns of (a) Co and (c) CoO. SEM images of (b) Co and (d) CoO.

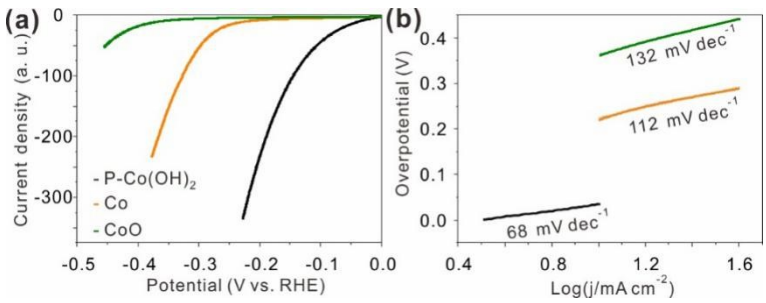

Fig. S9 (a) LSV curves and (b) corresponding Tafel plots of Co, CoO, and P-Co(OH)$_2$.

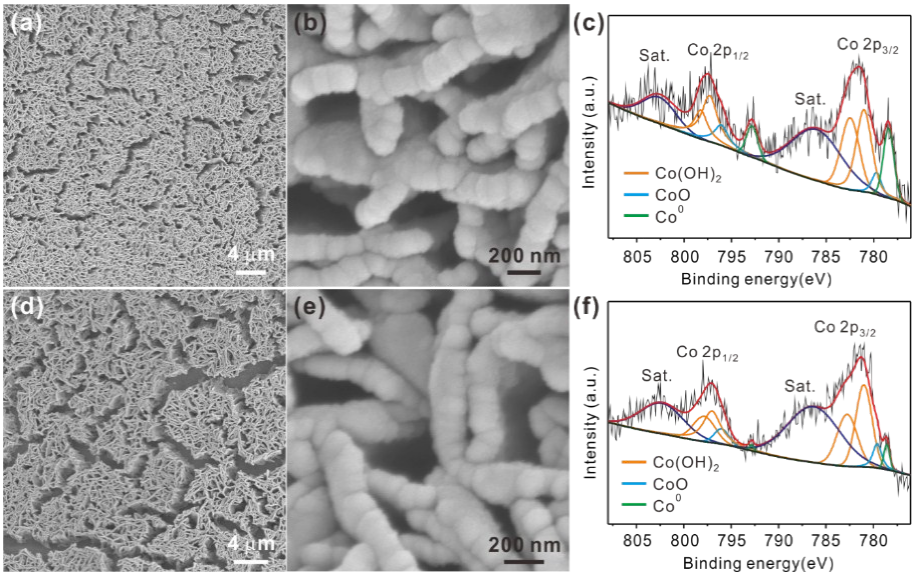

Fig. S10 (a,b) SEM images and (c) Co 2p XPS spectra of P-Co(OH)$_2$-3/7. (d,e) SEM images and (f) Co 2p XPS spectra of P-Co(OH)$_2$-1/1.

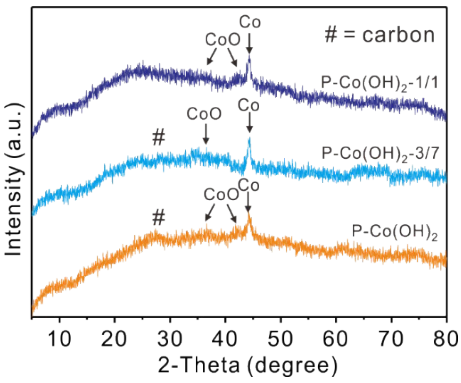

Fig. S11 XRD patterns of P-Co(OH)$_2$-1/1, P-Co(OH)$_2$-3/7 and P-Co(OH)$_2$.

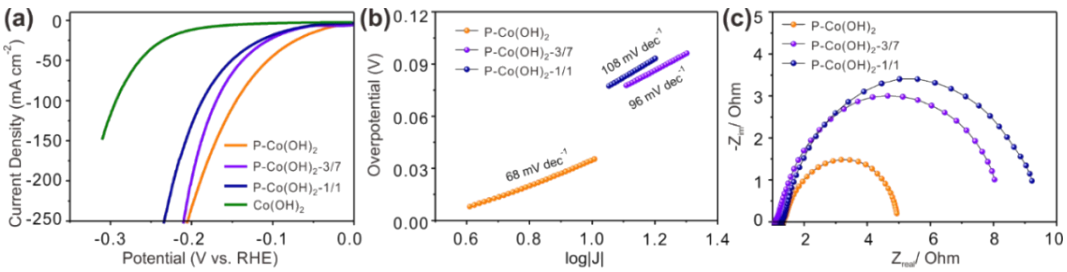

Fig. S12 (a) Polarization curves P-Co(OH)$_2$-1/1, P-Co(OH)$_2$-3/7, P-Co(OH)$_2$ and Co(OH)$_2$ at a scan rate of 2 mV s^{-1} of. (b) Tafel and (c) Nyquist plots of P-Co(OH)$_2$-1/1, P-Co(OH)$_2$-3/7, and P-Co(OH)$_2$.

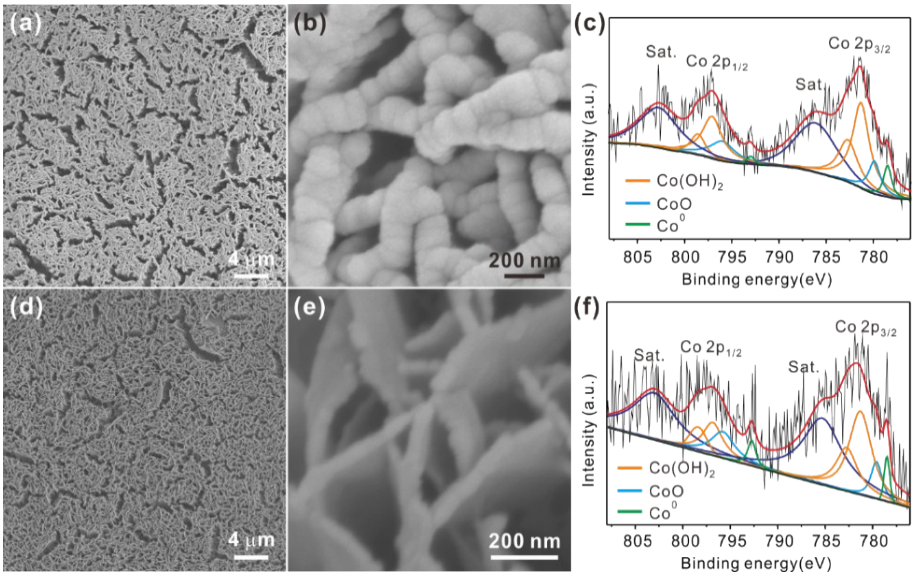

Fig. S13 (a,b) SEM images and (c) Co 2p XPS spectra of P-Co(OH)$_2$-20 Pa. (d,e) SEM images and (f) Co 2p XPS spectra of P-Co(OH)$_2$-60 Pa.

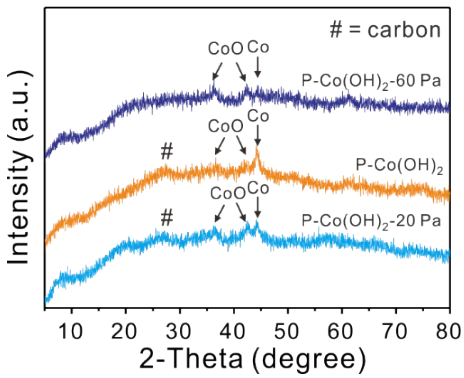

Fig. S14 XRD patterns of P-Co(OH)$_2$-20 Pa, P-Co(OH)$_2$-60 Pa, and P-Co(OH)$_2$.

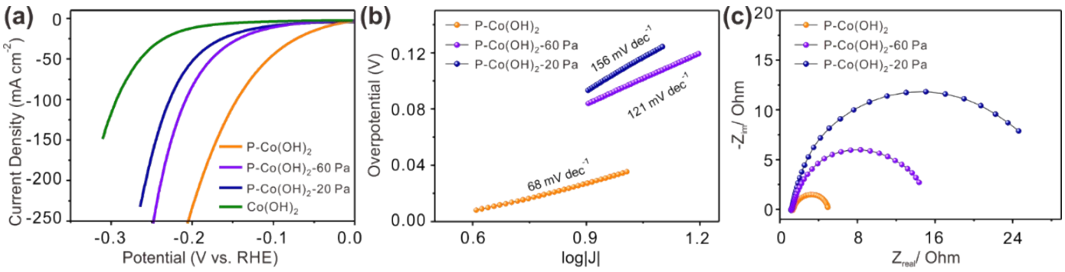

Fig. S15 (a) Polarization curves of P-Co(OH)$_2$-20 Pa, P-Co(OH)$_2$-60 Pa, P-Co(OH)$_2$ and Co(OH)$_2$ at a scan rate of 2 mV s^{-1}. (b) Tafel and (c) Nyquist plots of P-Co(OH)$_2$-20 Pa, P-Co(OH)$_2$-60 Pa, and P-Co(OH)$_2$.

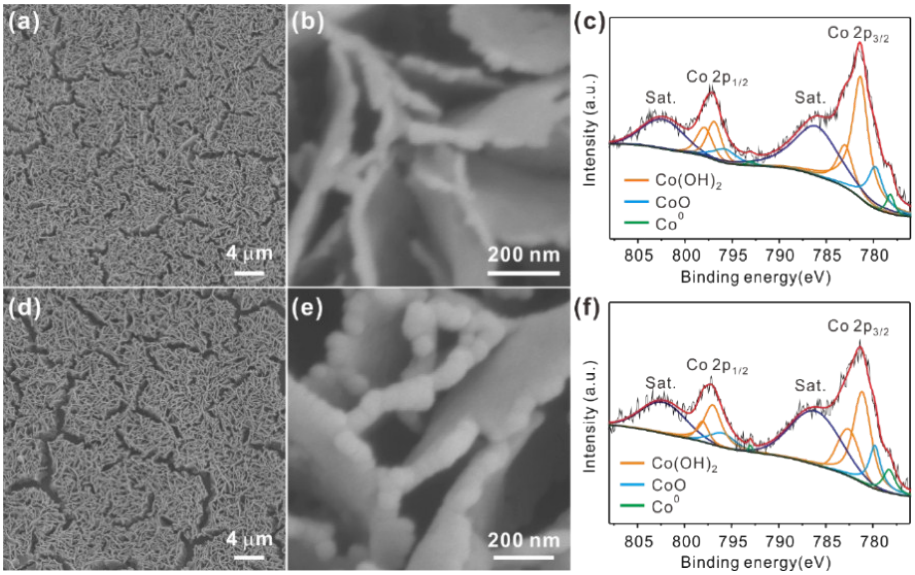

Fig. S16 (a,b) SEM images and (c) Co 2p XPS spectra of P-Co(OH)$_2$-200 W. (d,e) SEM images and (f) Co 2p XPS spectra of P-Co(OH)$_2$-300 W.

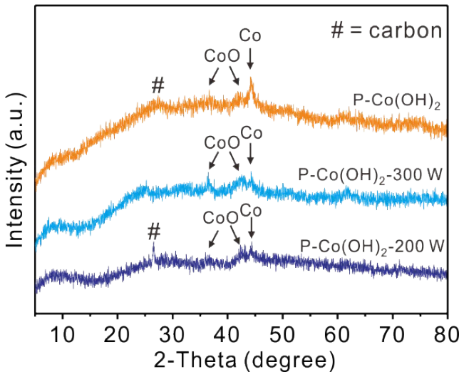

Fig. S17 XRD patterns of P-Co(OH)$_2$-200 W, P-Co(OH)$_2$-300 W, and P-Co(OH)$_2$.

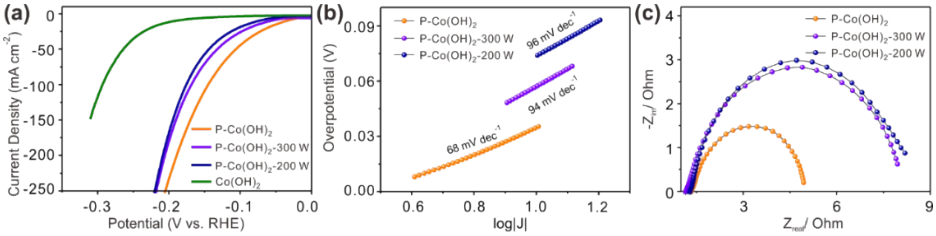

Fig. S18 (a) Polarization curves of P-Co(OH)$_2$-200 W, P-Co(OH)$_2$-300 W, P-Co(OH)$_2$ and Co(OH)$_2$ at a scan rate of 2 mV s^{-1}. (b) Tafel and (c) Nyquist plots of P-Co(OH)$_2$-200 W, P-Co(OH)$_2$-200 W, and P-Co(OH)$_2$.

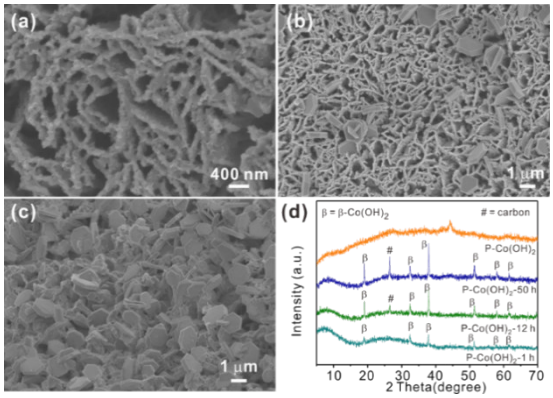

Fig. S19 SEM images of P-Co(OH)$_2$ after (a) 1 h, (b) 12 h, and (c) 50 h of stability test at the overpotential of 68 mV. (d) Time sequential XRD patterns of P-Co(OH)$_2$ during CA test.

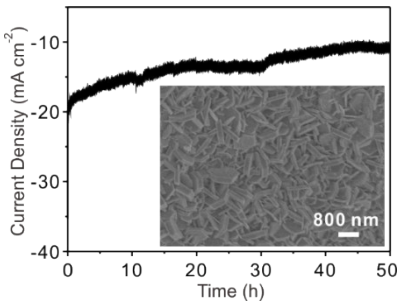

Fig. S20 The stability test of α-Co(OH)$_2$. The inset is the SEM image of Co(OH)$_2$ after 50 h of CA test at the overpotential of 220 mV in 1.0 M KOH.

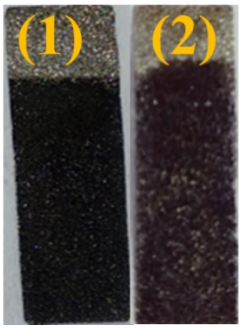

Fig. S21 The optical photograph of (1) P-Co(OH)$_2$-50 h, (2) Co(OH)$_2$-50 h.

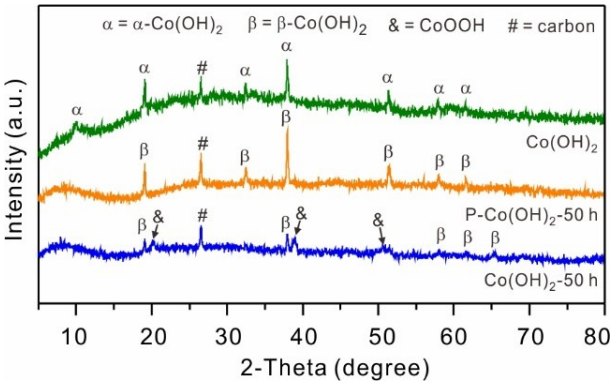

Fig. S22 XRD patterns of $Co(OH)_2$, P-$Co(OH)_2$-50 h, and $Co(OH)_2$-50 h

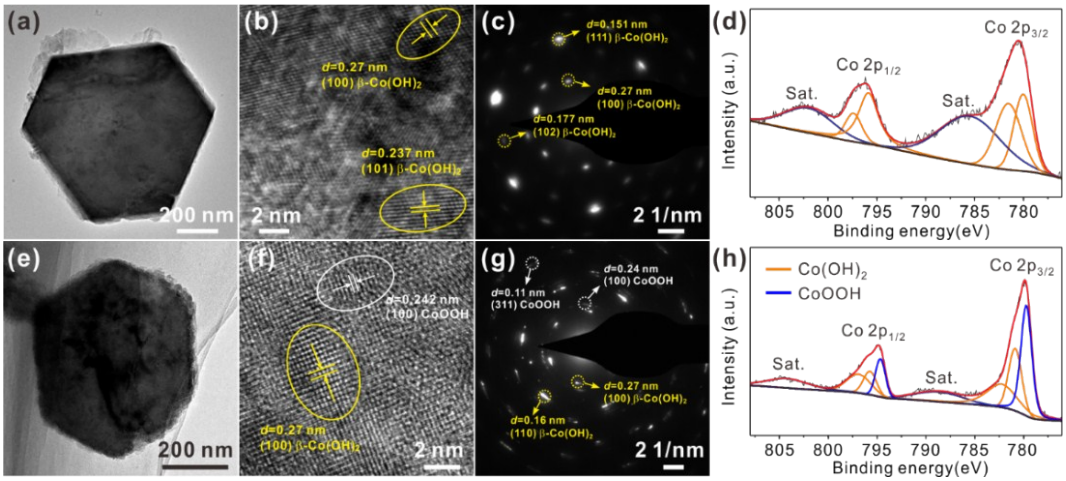

Fig. S23 (a) TEM image, (b) HRTEM image, (c) SAED pattern, and (d) Co 2p XPS spectra of P-$Co(OH)_2$-50 h. (e) TEM image, (f) HRTEM image, (g) SAED image, and (h) Co 2p XPS spectra of $Co(OH)_2$-50 h.

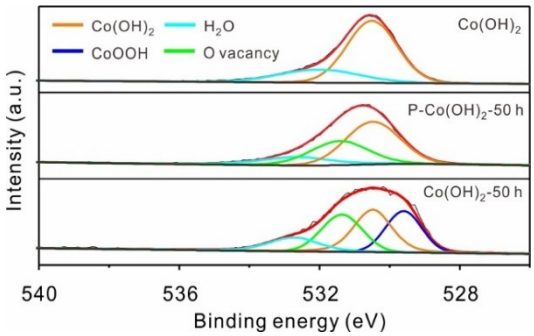

Fig. S24 O 1s XPS spectra of $Co(OH)_2$, P-$Co(OH)_2$-50 h, and $Co(OH)_2$-50 h.

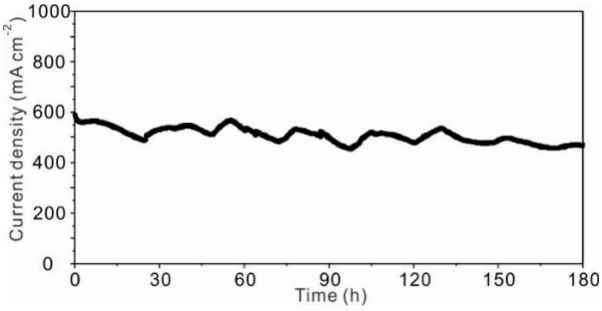

Fig. S25 CA test of P-$Co(OH)_2$ at 2.3 V.

Table S1 Comparison of the overall water splitting performance of P-$Co(OH)_2$ with other reported electrocatalysts in alkaline electrolyte.

Electrocatalysts	**Cell voltage (V@10 mA cm^{-2})**	**Ref.**
P-$Co(OH)_2$	**1.48**	**This work**
Ni_2P/Ni/NF	1.49	1
CoFePO/NF	1.564	2
NiCoP/rGO	1.59	3
CoP_2/RGO	1.56	4
NiCoP/NF	1.58	5
Ni,Zn dual-doped CoO NRs/CFP	1.52	6
Co_3O_4 NRs/NF	1.63	7
$NiFeO_x$/CFP	1.51	8
FeCoNi-ATNs/NF	1.55	9

Reference

1. B. You, N. Jiang, M. L. Sheng, M. W. Bhushan and Y. J. Sun, *ACS Catal.*, 2016, **6**, 714-721.
2. J. J. Duan, S. Chen, A. Vasileff and S. Z. Qiao, *ACS Nano*, 2016, **10**, 8738-8745.
3. J. Y. Li, M. Yan, X. M. Zhou, Z. Q. Huang, Z. M. Xia, C. R. Chang, Y. Y. Ma and Y. Q. Qu, *Adv. Funct. Mater.*, 2016, **26**, 6785-6796.
4. J. M. Wang, W. R. Yang and J. Q. Liu, *J. Mater. Chem. A*, 2016, **4**, 4686-4690.
5. H. F. Liang, A. N. Gandi, D. H. Anjum, X. B. Wang, U. Schwingenschlogl and H. N. Alshareef, *Nano Lett.*, 2016, **16**, 7718-7725.
6. T. Ling, T. Zhang, B. H. Ge, L. L. Han, L. R. Zheng, F. Lin, Z. R. Xu, W. B. Hu, X. W. Du, K. Davey and S. Z. Qiao, *Adv. Mater.*, 2019, **31**, 1807771.
7. H. T. Wang, H. W. Lee, Y. Deng, Z. Y. Lu, P. C. Hsu, Y. Y. Liu, D. C. Lin and Y. Cui, *Nat. Commun.*, 2015, **6**. 7261.
8. Y. P. Zhu, T. Y. Ma, M. Jaroniec and S. Z. Qiao, *Angew. Chem. Int. Ed.*, 2017, **56**, 1324-1328.
9. Q. R. Zhang, N. M. Bedford, D. Pan, X. Y. Lu and R. Amal, *Adv. Energy Mater.*, 2019, **9**, 1901312.